

$H \rightarrow \tau\tau$, CP measurement

IRN TERASCALE 06/11/20

Guillaume Bourgatte

Introduction

$$L_Y = -g_\tau (\cos(\phi_{\tau\tau}) \bar{\tau} \tau + \sin(\phi_{\tau\tau}) \bar{\tau} i \gamma_5 \tau) h$$

$\phi_{\tau\tau} = 0 \rightarrow$ scalar (SM)

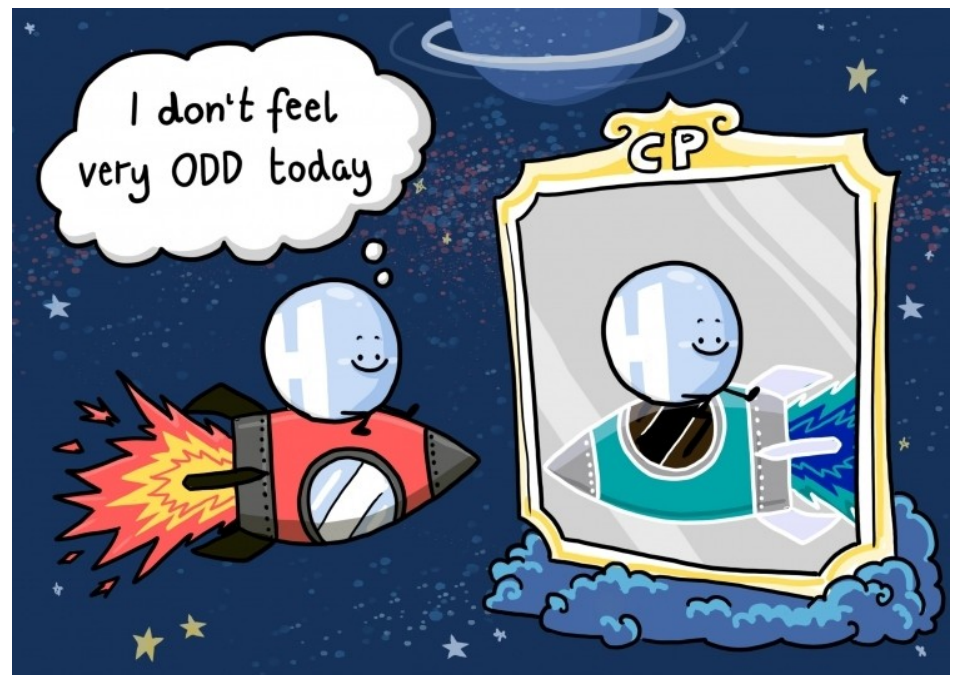
$\phi_{\tau\tau} = \pi/2 \rightarrow$ pseudoscalar

$0 < \phi_{\tau\tau} < \pi/2 \rightarrow$ mixed state with CP violation \rightarrow maximal violation for $\phi_{\tau\tau} = \pi/4$

Pseudoscalar state excluded from measurements made in decays into electroweak bosons

(*Phys. Rev. Lett.* 110 (2013) no.8)

3 signal templates used in the analysis



A view of the Higgs boson in a CP mirror (image: DESY/designdoppel)

Outline

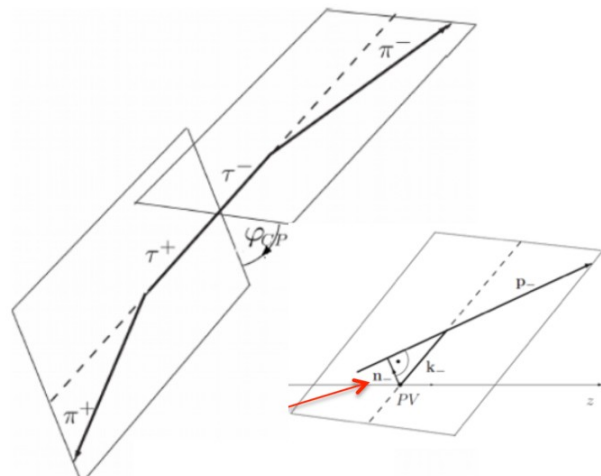
- **First part:** first CMS results based on Run 2 ([CMS-PAS-HIG-20-006](#), [physics briefing](#))
- **Second part:** polarimetric vector method in the 3prongs*3prongs ($a_1^{3\text{pr}} a_1^{3\text{pr}}$) channel

Methods

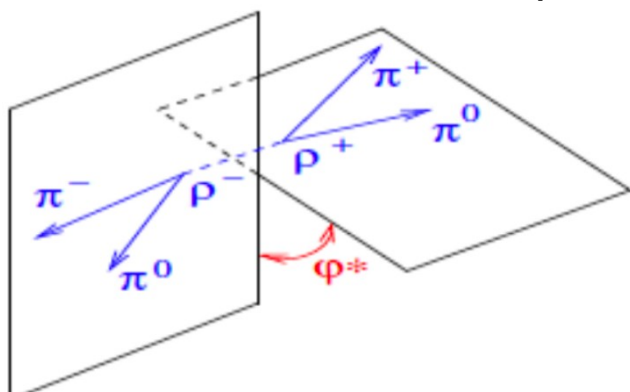
$e^- \bar{v}_e v_\tau$	$\mu^- \bar{v}_\mu v_\tau$	$\pi^\pm v_\tau$	$\rho^\pm v_\tau \rightarrow \pi^\pm \pi^0 v_\tau$	$a_1^{1pr} v_\tau \rightarrow \pi^\pm 2\pi^0 v_\tau$	$a_1^{3pr} v_\tau \rightarrow 3\pi^\pm v_\tau$
17.8%	17.4%	10.8%	25.5%	9.3%	9.0%

Impact parameter vector method:

Use IP to define tau direction



Decay plane method: Use decay products to reconstruct tau planes



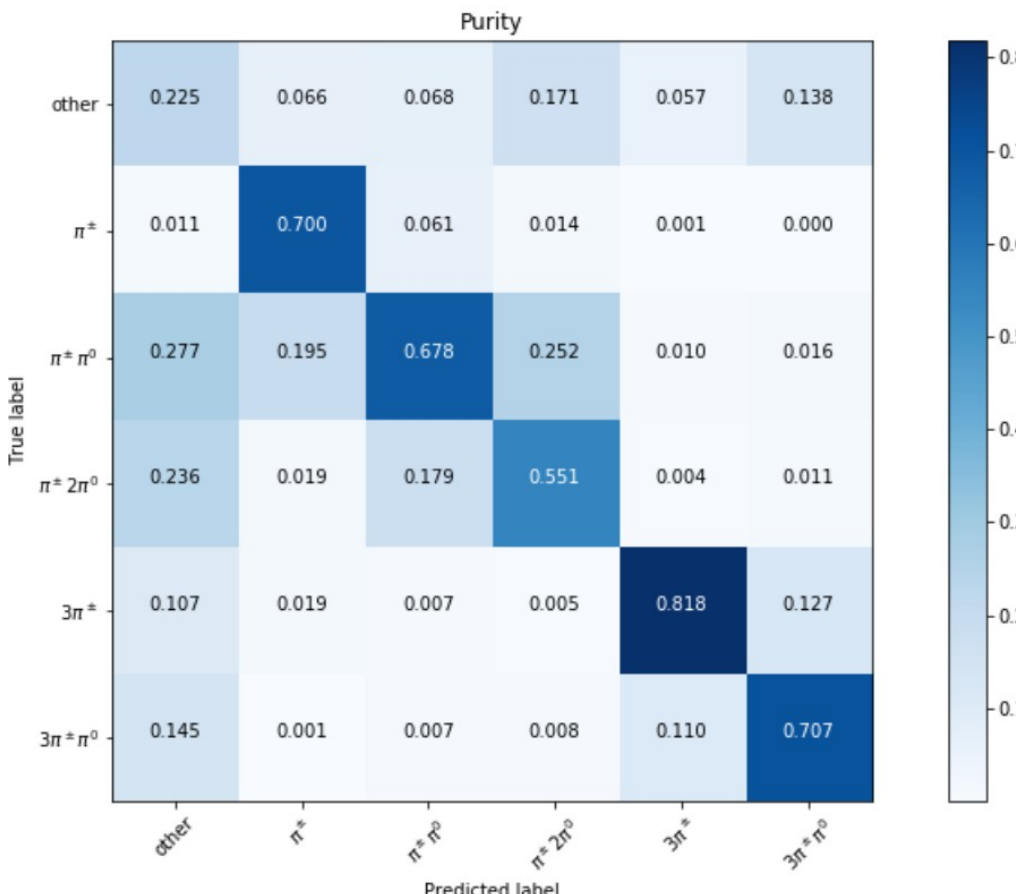
$\tau_h \tau_h$
 $\rho + \rho$ (DP-DP)
 $a_1^{1pr} + \rho$ and $a_1^{1pr} + a_1^{1pr}$ (DP-DP)
 $a_1^{3pr} + \rho$ (DP-IP)
 $a_1^{3pr} + a_1^{3pr}$ (DP-DP)
 $\rho + \pi^\pm$ (DP-IP)
 $\pi^\pm + \pi^\pm$ (IP-IP)
 $a_1^{3pr} + \pi^\pm$ (DP-IP)
 $a_1^{1pr} + \pi^\pm$ (DP-IP)
 $a_1^{3pr} + a_1^{1pr}$ (DP-DP)

$\mu \tau_h$
 $\mu + \rho$ (IP-DP)
 $\mu + \pi^\pm$ (IP-IP)
 $\mu + a_1$ (IP-DP)
 $\mu + a_1^{1pr}$ (IP-DP)

 $e \tau_h$
 $e + \rho$ (IP-DP)
 $e + \pi^\pm$ (IP-IP)
 $e + a_1$ (IP-DP)
 $e + a_1^{1pr}$ (IP-DP)

Tau decay mode identification

Hadron-Plus-Strip (HPS) decay mode classification replaced by MVA decay mode classification (BDT) exploiting the features of τ_h decay products (HPS decay mode, angular variables, kinematic quantities, etc...)



purity confusion matrix

Efficiency and Purity tables comparing HPS DM and MVA DM methods across various decay channels.

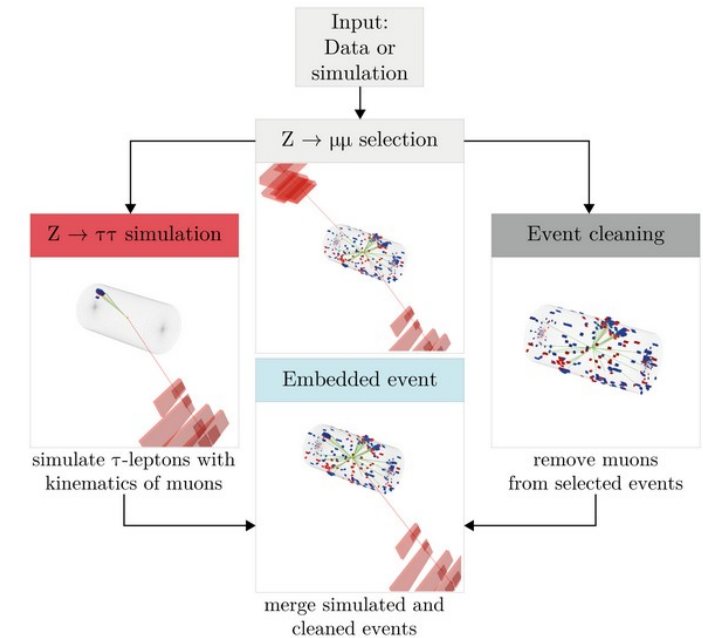
	π	$\pi\pi^0$	$\pi 2\pi^0$	3π	$3\pi\pi^0$
HPS DM	75%	73%	0%	89%	53%
MVA DM	83%	79%	39%	87%	65%
Gain	8%	6%	39%	-2%	12%

	π	$\pi\pi^0$	$\pi 2\pi^0$	3π	$3\pi\pi^0$
HPS DM	56%	56%	0%	67%	55%
MVA DM	70%	68%	55%	82%	71%
Gain	14%	12%	55%	15%	16%

Background estimation

Z → ττ: data-driven background estimation for the Zττ background (embedding method):

- Z → μμ events selected in data
- The two muon tracks as well as their calorimetry entries removed from the event
- The kinematics of the di-muon system used to simulate a Z → ττ decay with those same kinematics
- Cleaned and simulated events merged to form a hybrid embedded event



Advantages:

- Better description of jets, pile-up, detector noise and resolution effects
- Less corrections needed compared to Monte Carlo (e.g. no recoil, jet energy scale or btag scale factors)

Background estimation

jet → τ_h : estimation in signal region (SR) obtained by reweighting events in side-band regions (application regions, AR) in data where the leading τ_h candidates fails Medium DeepTau ID Working Point (WP) but passes VeryVeryVeryLoose WP

Weights measured in derivation region (DR) enriched in jet → τ_h :

$$FF = \frac{N(\text{Medium})}{N(\text{VVVLoose \& ! Medium})}$$

$\tau_h\tau_h$
DR for QCD = same-sign $\tau\tau$ pair

$I\tau_h$
DR for QCD = same-sign and $I_{\text{rel}}^{\ell} > 0.05$
DR for W+jets = mT>70 GeV
Top-antitop subtracted using MC

Event categorisation

- DNN for $\mu\tau_h$ and BDT for $\tau_h\tau_h$
- 3 categories: **Higgs, $Z\tau\tau$ embedded and jet $\rightarrow \tau_h$ fakes**
- ggH and VBF categories merged
- Input variables comprise most important subset of variables used in SM ML analysis:

$\mu\tau_h$

- leading $\tau_h p_T$;
- visible di-tau p_T ;
- full di-tau + MET p_T ;
- visible di- τ_h mass;
- SVfit mass;
- leading jet p_T ;
- MET;
- number of jets;
- invariant mass of di-jet system.

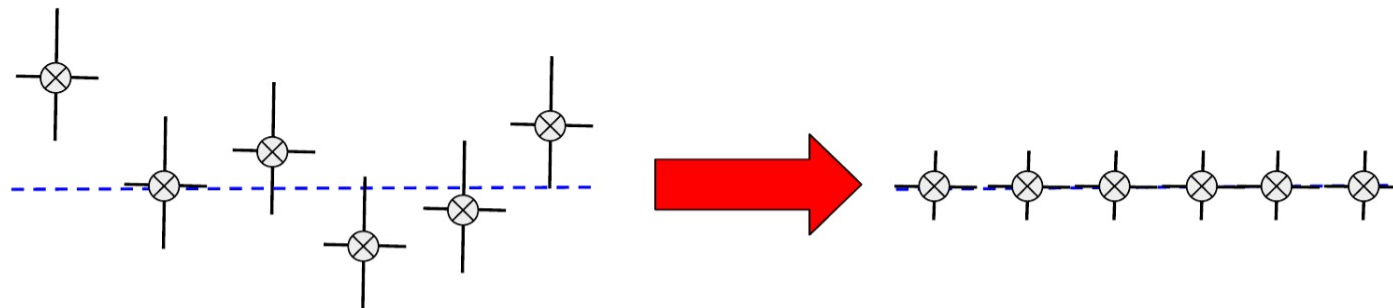
$\tau_h\tau_h$

- muon p_T ;
- Tau lepton p_T ;
- Combined p_T of muon, tau and missing transverse momentum;
- Number of jets
- P_T of the leading jet;
- P_T of the trailing jet;
- Combined P_T for the two leading jets;
- Invariant mass of the two leading jets;
- Separation in pseudorapidity between the two leading jets;
- Visible invariant di-tau mass;
- Invariant di-tau mass obtained with FastMTT algorithm;
- MET;
- Transverse mass of the muon and MET system.

Background smoothing

Due to the nature of the acoplanarity angle (symmetric by construction) we can exploit symmetries in the bkg processes to reduce statistical fluctuations in MC:

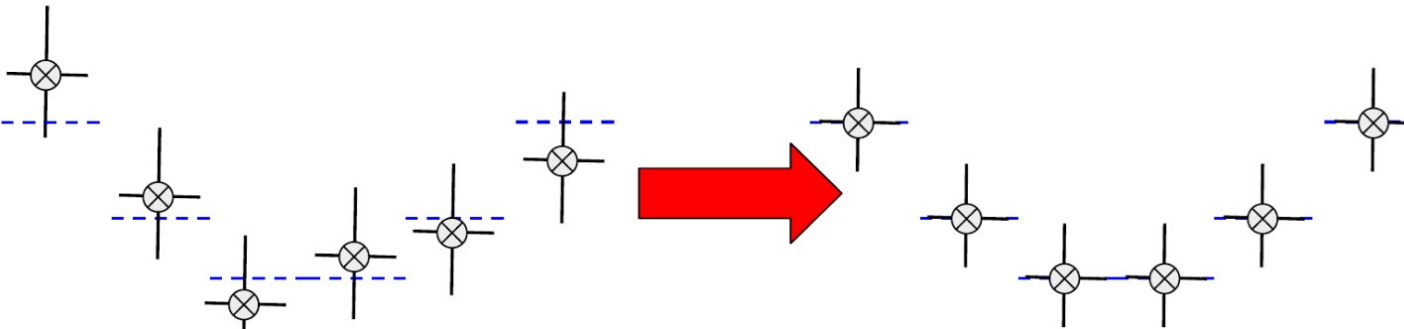
Most backgrounds are flat in the absence of reconstruction-level smearing



Flattening

Used for processes with genuine taus or $\ell \rightarrow \tau$ fakes

$\pi + \pi$ and $\mu + \pi$ have correlated smearing due to PV

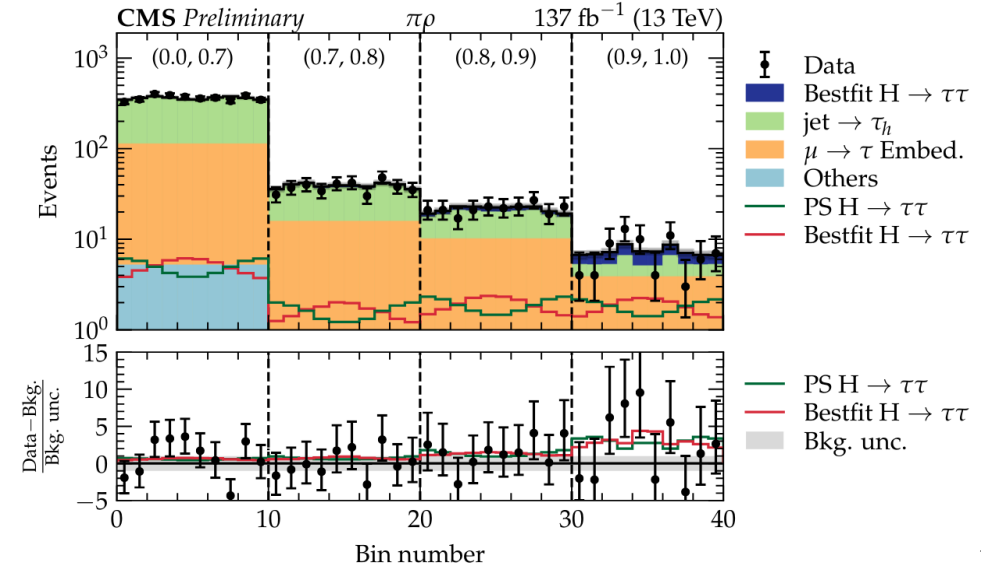
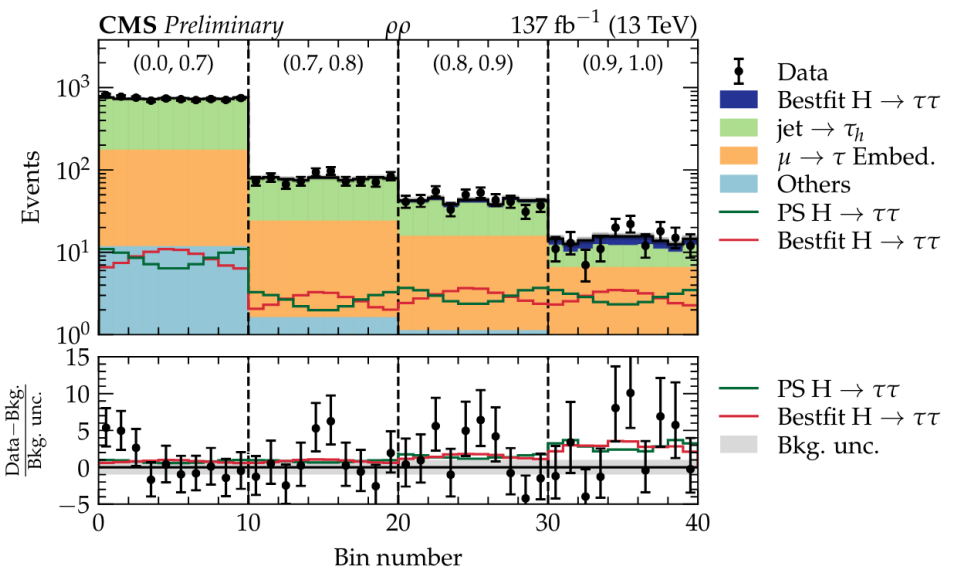
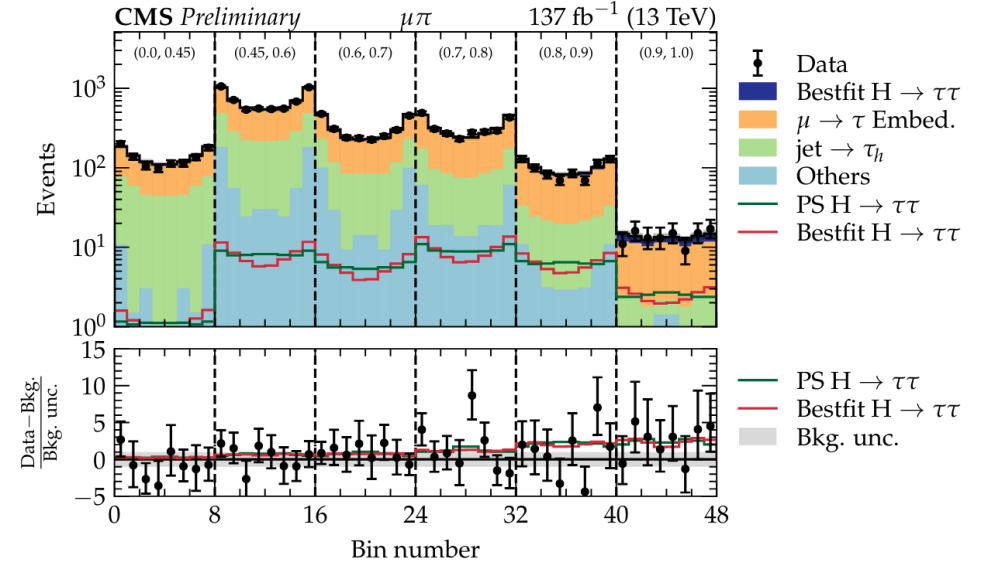
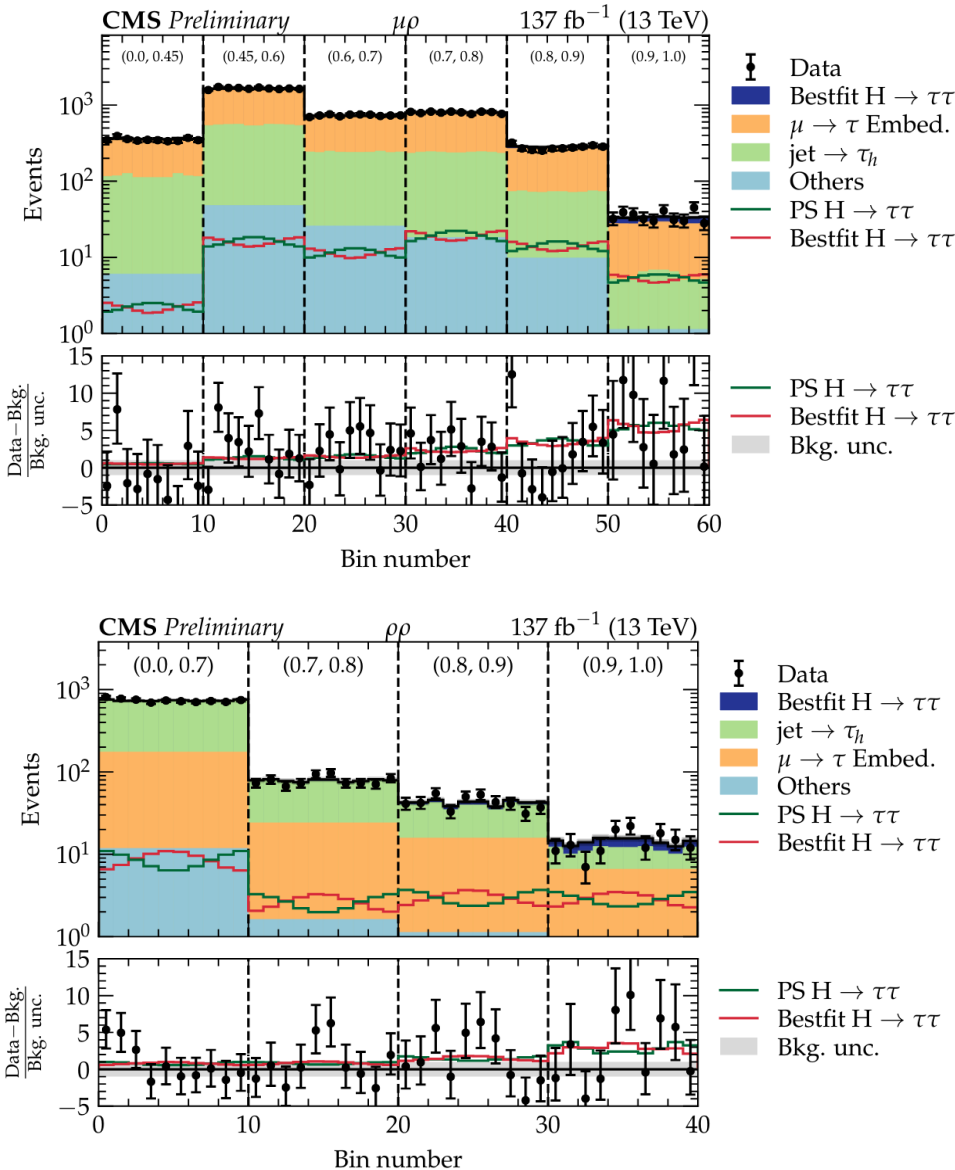


Symmetrising

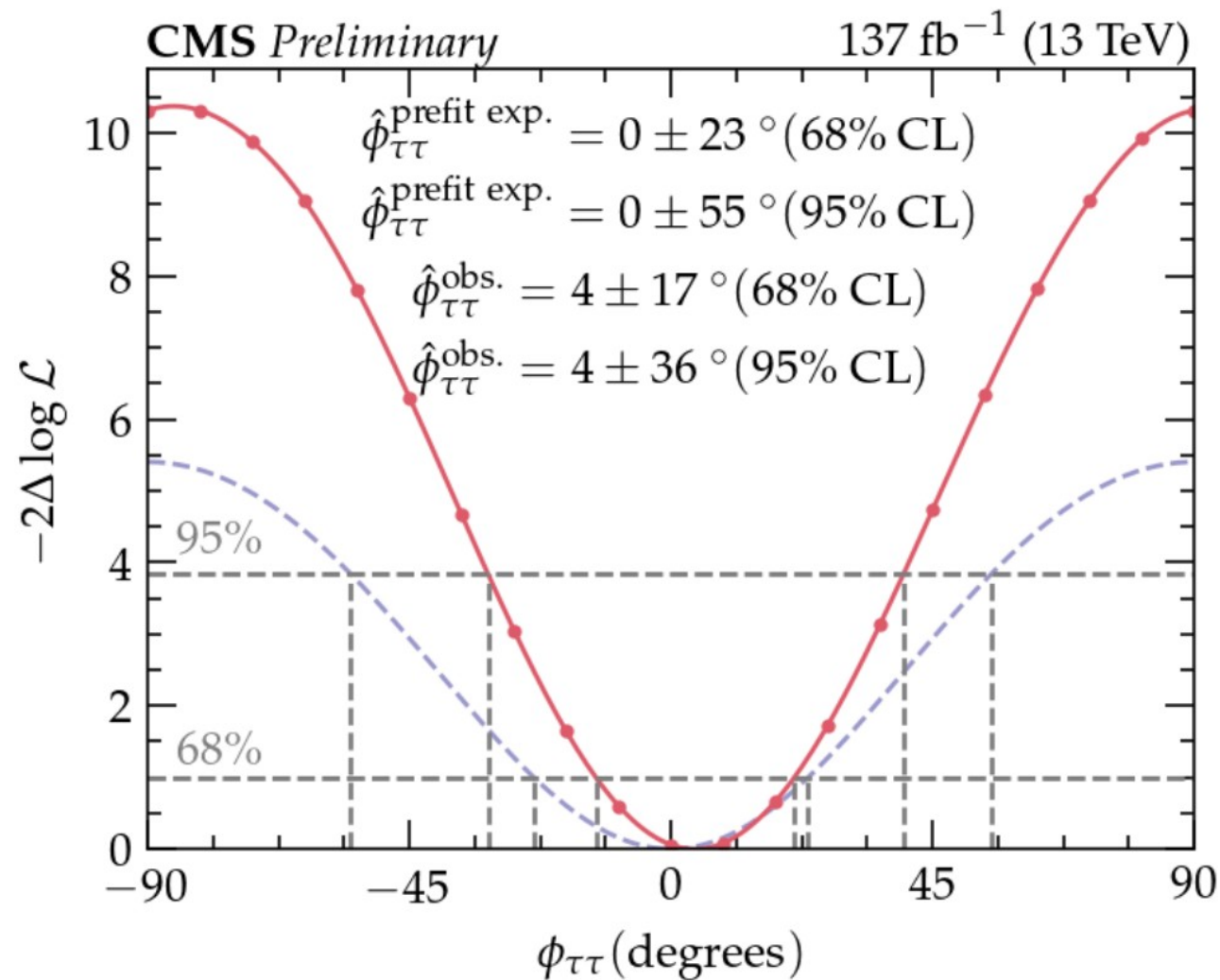
Used for processes with $j \rightarrow \tau$ fakes or IP method

Signal: scalar and pseudoscalar templates symmetrized w.r.t π but maximally mixed template ($\phi_{\pi\pi} = \pi/4$) anti-symmetrized

Postfit distributions – signal categories



Results



$$\Phi_\pi = (4 \pm 17 \text{ (stat)} \pm 2 \text{ (bin-by-bin)} \pm 1 \text{ (syst)} \pm 1 \text{ (theory)})^\circ$$

**2.3 σ expected
3.2 σ observed**

CMS-PAS-HIG-20-006

Illustrative ϕ_{CP} plot

Most sensitive channels: $\rho\rho + \pi\rho + \mu\rho$

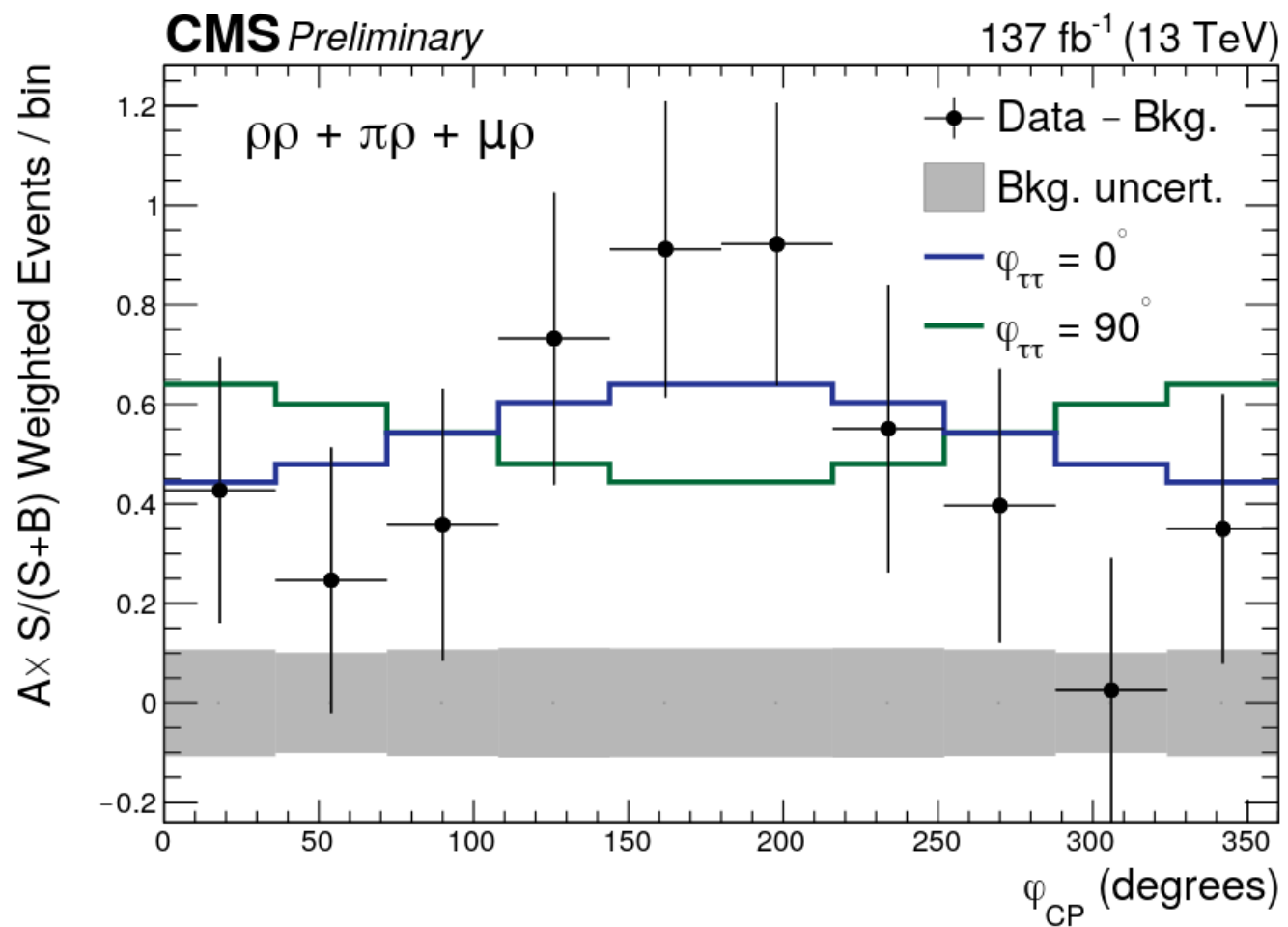
Bins reweighted by $(A^*S/(S+B))/Nbins$:

- S=signal
- B=background
- $A = \frac{|CP^{even} - CP^{odd}|}{|CP^{even} + CP^{odd}|}$

Background is subtracted from the data

Grey uncertainty band indicates the uncertainty on the subtracted background component

The data clearly favour the CP-even hypothesis, CP-odd hypothesis excluded with 3.2 standard deviations



$a_1^{3\text{pr}}$ $a_1^{3\text{pr}}$ channel

- The decay plane method is usually used for the $a_1^{3\text{pr}}a_1^{3\text{pr}}$ channel
- This channel allows us to reconstruct the Higgs rest frame thanks to presence of tau secondary vertices (SV)
- Although its not very significant channel we can do better with the polarimetric vector method

Polarimetric vector

For any τ decay, the differential decay width (τ rest frame) can be written as: $d\Gamma \propto (1 + \vec{h} \cdot \vec{S})$

\vec{h} : "polarimetric vector", given by the kinematics of the decay in the τ rest frame

\vec{S} : τ spin vector

$d\Gamma$ is maximal for \vec{h} oriented along $\vec{S} \rightarrow \vec{h}$ most likely points in the direction of \vec{S}

\vec{h} is hence the best estimate of the direction of \vec{S}

Polarimetric vector definition vs decay mode

$$\tau^\pm \rightarrow \pi^\pm \nu : \vec{h} = -\vec{n}_\pi$$

$$\tau^\pm \rightarrow \rho^\pm \nu \rightarrow \pi^\pm \pi^0 \nu : \vec{h} = m_\tau \frac{2(qN)\vec{q} - q^2 \vec{N}}{2(qN)(qP) - q^2(NP)}$$

m_τ : τ mass

q : $\pi^\pm - \pi^0$

N : $\nu = \tau^\pm - \pi^\pm - \pi^0$

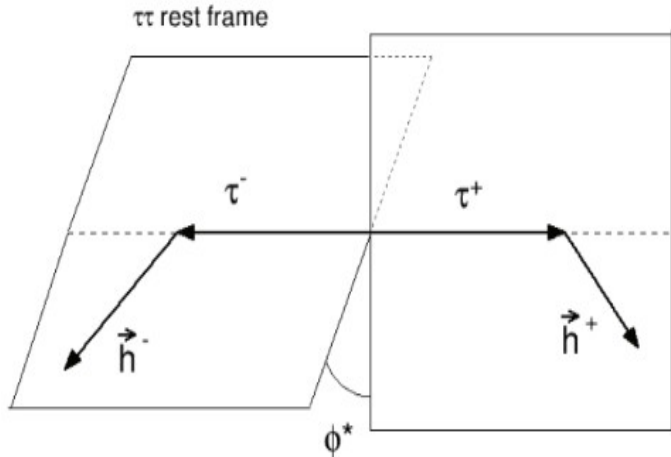
P : τ^\pm

4-vectors

Complex for 3 prongs decay

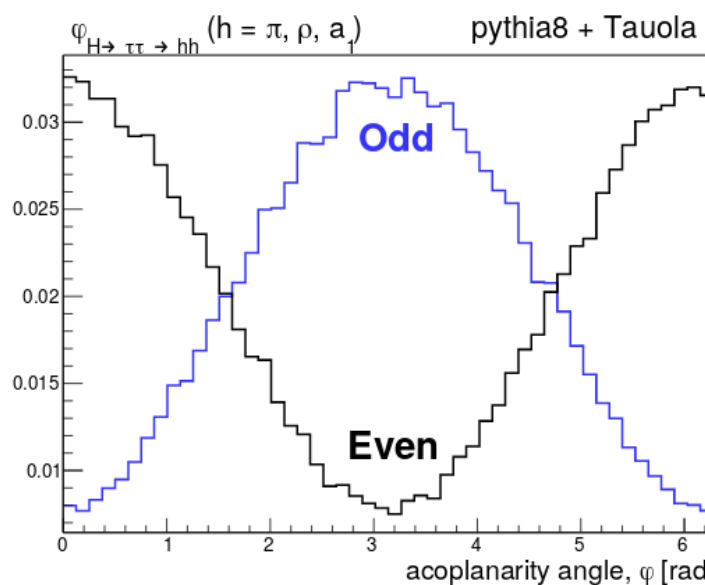
Parametrization from the CLEO collaboration (*Phys. Rev. D61* (2000) 012002) taking into consideration the resonance decay model

Polarimetric vector method



An acoplanarity angle can be built using the direction of taus and polarimetric vectors (in the Higgs rest frame)

$\vec{\tau}$: Unit vector pointing along the direction of the τ in the H rest frame
 \vec{h} : Polarimetric unit vector

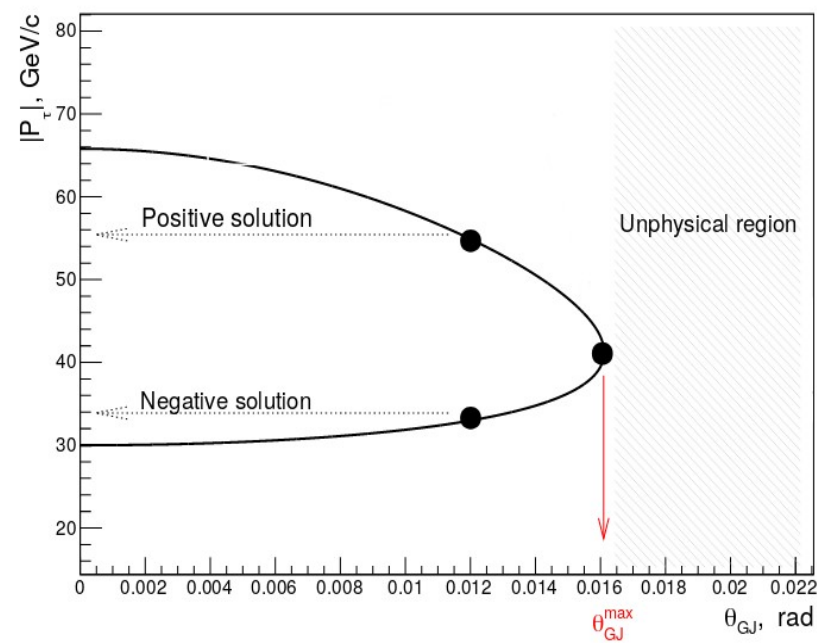
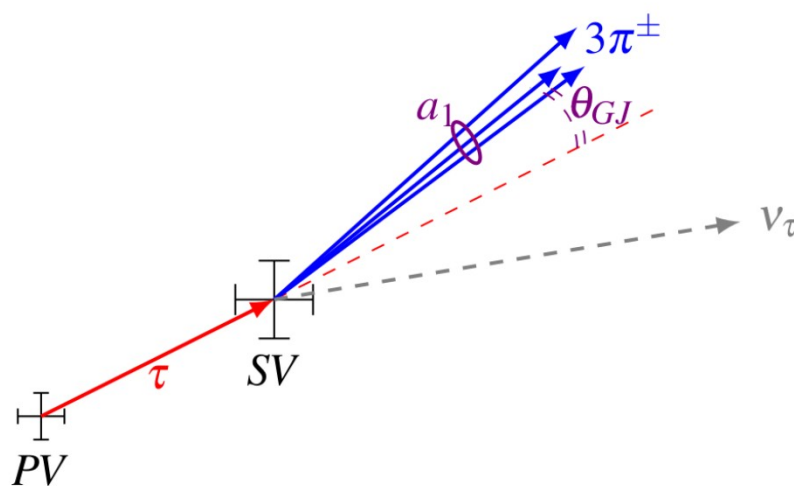


ArXiv:1811.03969
V. Cherepanov, E.
Richter-Was, and Z.
Was

Estimation of the tau 4-vector

Simplified approach of Global Event Fit (GEF) method: arXiv:1805.06988v2, V. Cherepanov and A. Zott (M2 internship C. Grimault)

τ momentum estimated using **energy and momentum conservation** with **massless neutrino** and θ_{GJ} **Gottfried-Jackson angle** (angle between a_1 and τ in lab frame)



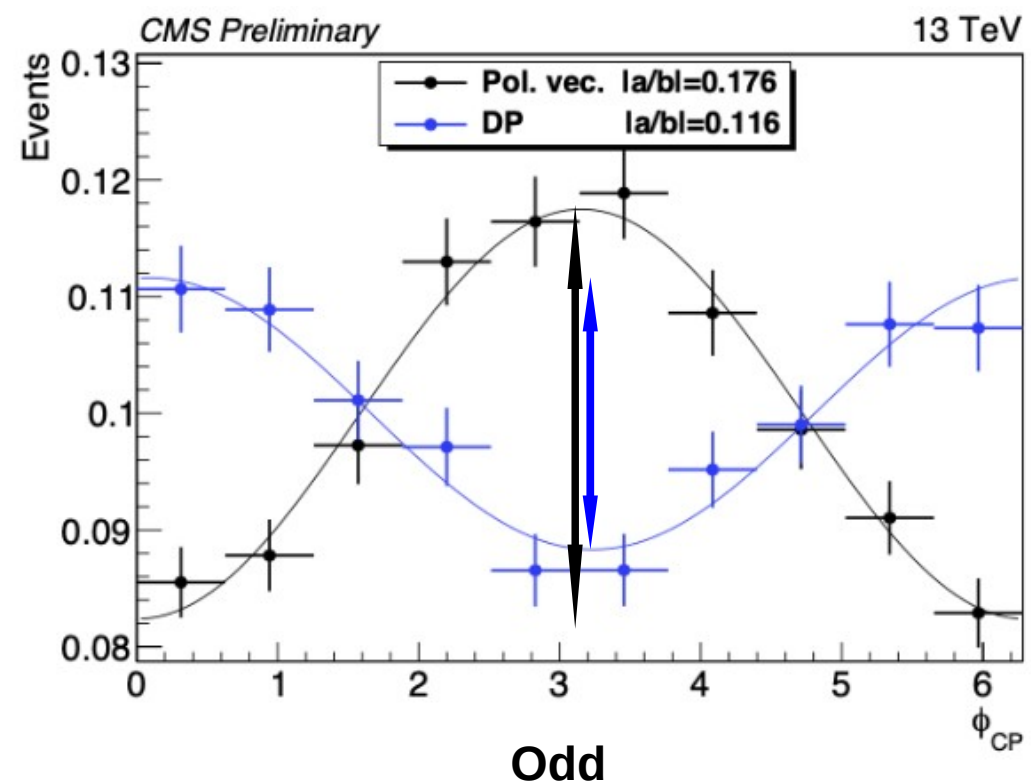
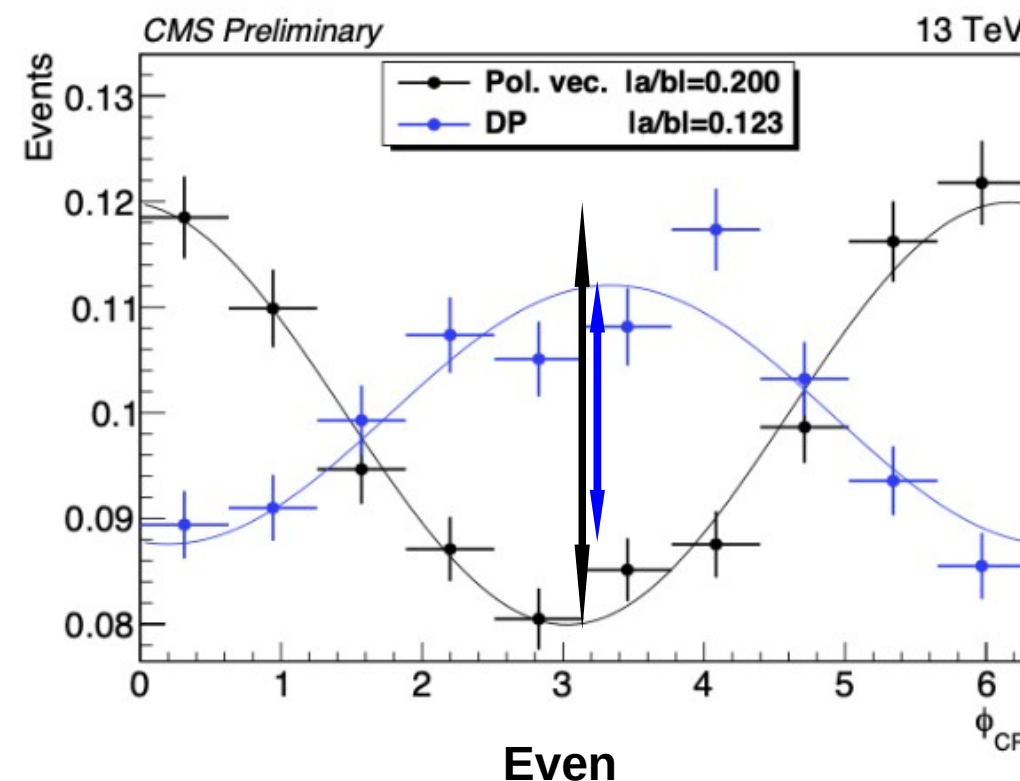
- Two possible solutions per tau
- If the event is in an unphysical region: $\theta_{GJ} \rightarrow \theta_{GJ}^{\max}$
- Ambiguity of the τ momentum \rightarrow **Pair with the closest invariant mass to M_H**
- **τ direction estimated with $\vec{SV} - \vec{PV}$**

ϕ_{CP} oscillations and comparison with decay plane

Different conventions between decay plane and pol. vec. method \rightarrow extrema shifted

Fit:
 $b+a\cos(\varphi+x)$

a: amplitude
b: baseline
 φ : phase



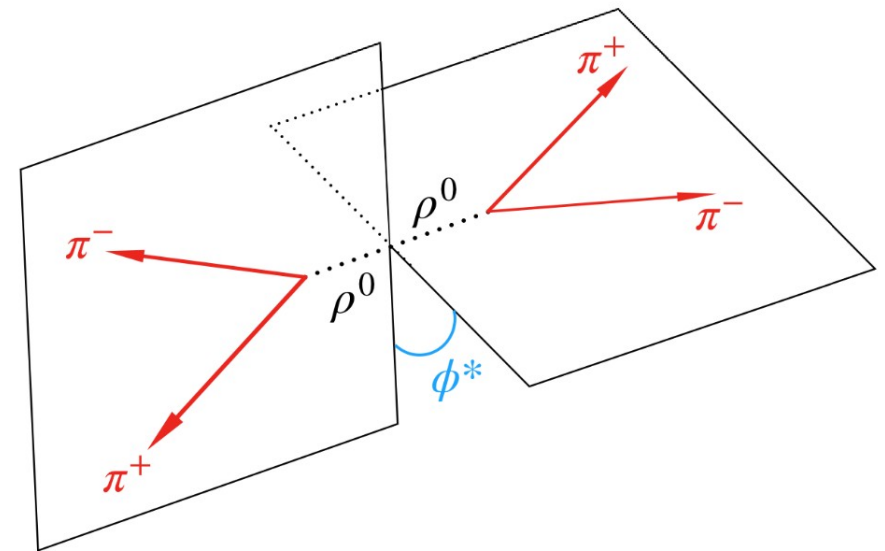
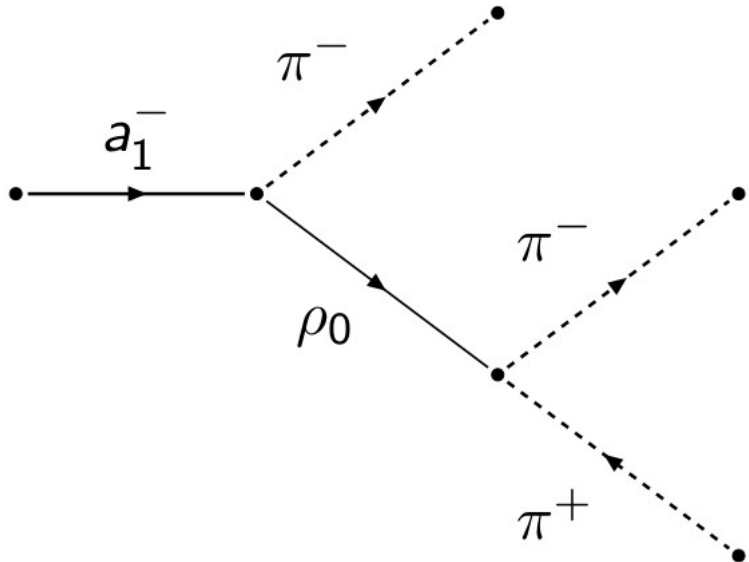
Conclusion

- First measurement of the CP structure of the tau Yukawa coupling
- Whole Run 2 (137 fb^{-1}) analysed
- Result: $\Phi_{\pi} = 4 \pm 17^\circ$
- The data clearly favour the CP-even hypothesis, CP-odd hypothesis excluded with 3.2 standard deviations
- The polarimetric vector method gives better CP states separation compared to the decay plane method used in the CMS analysis for the $a_1^{3\text{pr}}a_1^{3\text{pr}}$ channel, being unblinded
- Promising method that could be extended to other channels during Run 3 and HL-LHC

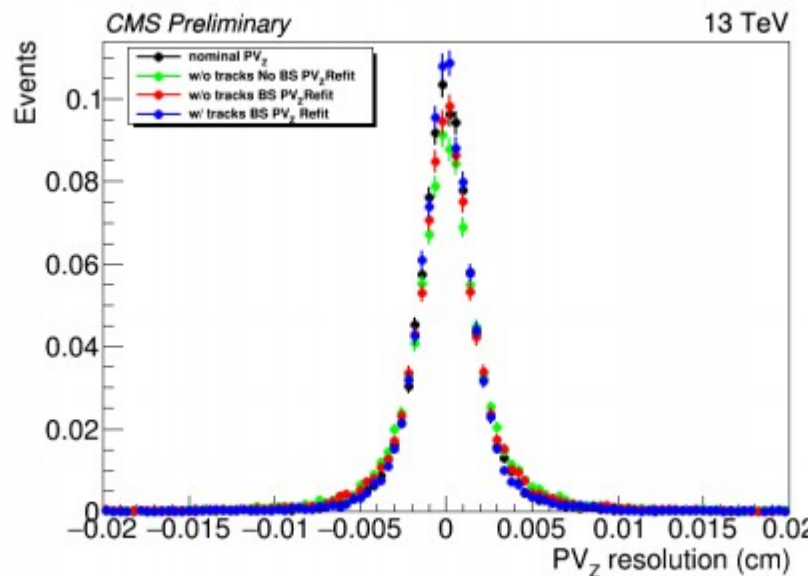
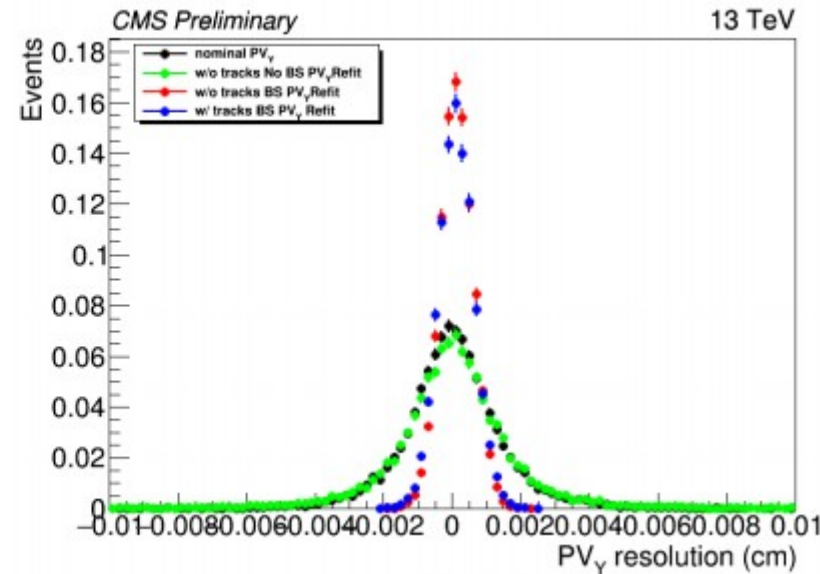
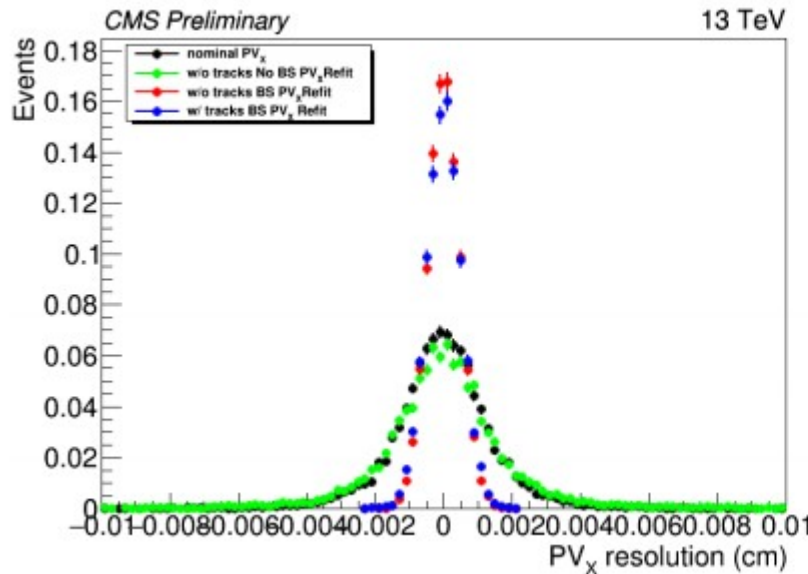
Backup

Decay plane method with 3 prongs

- $a_1^{3\text{pr}} v_\tau \rightarrow \rho^0 \pi^\pm v_\tau \rightarrow 3\pi^\pm v_\tau$
- Determine pions pair with mass closest to intermediate ρ
- Construct ρ decay plane



Refitted primary vertex



Primary vertex resolution in cm

Production mode	Vertex type	σ_x^{PV}	σ_y^{PV}	σ_z^{PV}
$H \rightarrow \tau_\mu \tau_h$	Nominal	17	17	26
	Refitted Beamspot-Corrected	5	5	29
$Z \rightarrow \tau_\mu \tau_h$	Nominal	20	20	30
	Refitted Beamspot-Corrected	5	5	34

The primary vertex has been adjusted w/ beam spot constraint and tau tracks excluded

Refitted primary vertex

Channel	year	Trigger requirement	Offline lepton selection		
			p_T (GeV)	η	Isolation
$\tau_h \tau_h$	all years	$\tau_h(35) \& \tau_h(35)$	$p_T^{\tau_h} > 40$	$ \eta^{\tau_h} < 2.1$	DNN τ_h ID
	2016	$\mu(22), \mu(19) \& \tau_h(20)$	$p_T^{\tau_h} > 20$	$ \eta^\mu < 2.1$	$I^\mu < 0.15$
$\tau_\mu \tau_h$	2017, 2018	$\mu(24), \mu(20) \& \tau_h(27)$	$p_T^{\tau_h} > 25$	$ \eta^{\tau_h} < 2.3$	DNN τ_h ID
			$p_T^{\tau_h} > 21$	$ \eta^\mu < 2.1$	$I^\mu < 0.15$
			$p_T^{\tau_h} > 32$	$ \eta^{\tau_h} < 2.3$	DNN τ_h ID

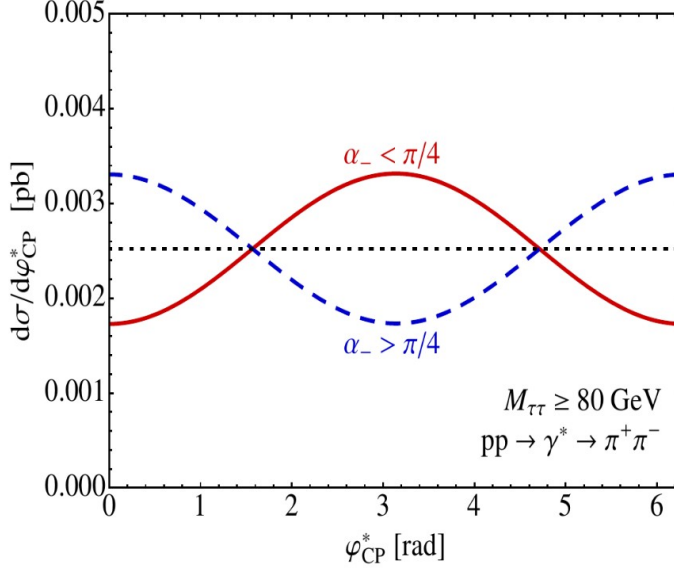
Kinematic trigger and offline requirements applied for the $\tau_\mu \tau_h$ and $\tau_h \tau_h$ channel. The pseudorapidity constraints originate from trigger and reconstruction requirements.

Z $\tau\tau$ validation

Validation performed by decomposing the ϕ_{CP} distributions in two categories:

- “nearly coplanar” taus
- “nearly perpendicular” taus

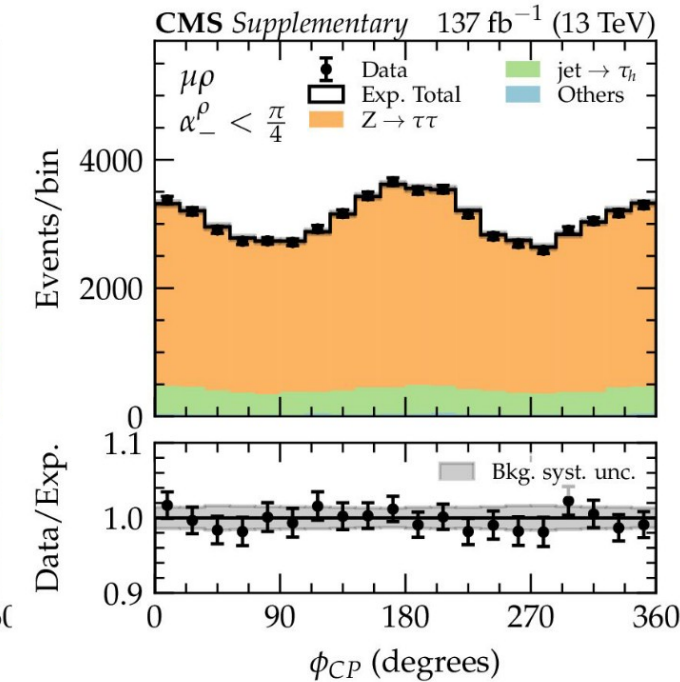
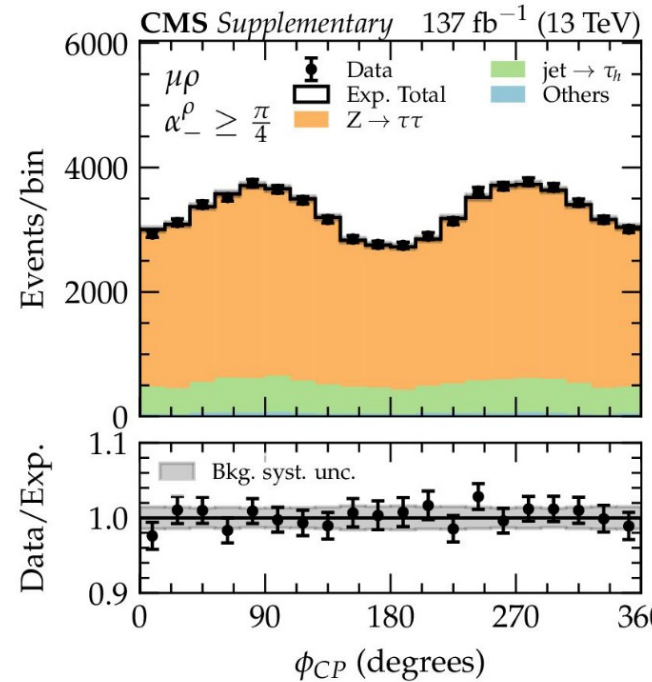
α_- allows to extract two contributions with a modulation in ϕ_{CP}



Stefan Berge et al.

$$\cos \alpha_- = \left| \frac{\hat{\mathbf{e}}_z \times \hat{\mathbf{p}}_{L-}}{|\hat{\mathbf{e}}_z \times \hat{\mathbf{p}}_{L-}|} \cdot \frac{\hat{\mathbf{n}}_- \times \hat{\mathbf{p}}_{L-}}{|\hat{\mathbf{n}}_- \times \hat{\mathbf{p}}_{L-}|} \right|$$

P_{L-} : π^- directions of flight in the laboratory frame
 e_z points along the direction of one of the proton beams
 n_- : impact parameter vectors in the laboratory frame



Shape systematics

Uncertainty	Magnitude	Correlation	Incorp. fit
τ_h ID	p_T /decay-mode dependent (2–3%)	no	Gaussian
Muon reconstruction	1%.	yes	log-normal
$e \rightarrow \tau_h$ ID	5(1)% 2016(2017,2018)	no	Gaussian
$\mu \rightarrow \tau_h$ ID	20–40%	no	Gaussian
μ ID	1%	yes	Gaussian
b-jet veto	1–9%	no	log-normal
Luminosity	2.5%	partial	log-normal
Trigger	2% for μ , p_T -dep. for τ_h	no	Gaussian
Embedded yield	4%	no	log-normal
$t\bar{t}$ cross section	4.2%	yes	log-normal
Diboson cross section	5%	yes	log-normal
Single top cross section	5%	yes	log-normal
$W + \text{jets}$ cross section	4%	yes	log-normal
Drell-Yan cross section	2%	yes	log-normal
Signal cross sections	[82]	yes	log-normal
top p_T reweighing	10%	yes	Gaussian
$Z p_T$ reweighing	10%	partial	Gaussian
Prefiring (2016, 2017)	Event-dependent (0–4%)	yes	log-normal
τ_h energy scale	1% (sim), 1.5% (emb.)	no	Gaussian
$e \rightarrow \tau_h$ energy scale	0.5–6.5%	no	log-normal
$\mu \rightarrow \tau_h$ energy scale	1%	no	log-normal
Muon energy scale	0.4–2.7%	yes	Gaussian
Jet energy scale	Event-dependent	partial	Gaussian
Jet energy resolution	Event-dependent	no	Gaussian
p_T^{miss} unclustered scale	Event-dependent	no	Gaussian
p_T^{miss} recoil corrections	Event-dependent	no	Gaussian
Jet $\rightarrow \tau_h$ mis-ID	described in text	partial	Gaussian
$t\bar{t}$ /diboson in embedded	10%	yes	Gaussian
S_{IP} in μ and π decays	25%	no	Gaussian

Expected sensitivities

Decay mode	Expected sensitivity
$\tau_\mu \tau_h$	1.47
$\mu\rho$	1.16
$\mu\pi$	0.71
μa_1^{3pr}	0.51
μa_1^{1pr}	0.24
$\tau_h \tau_h$	1.8
$\rho\rho$	1.09
$\rho\pi$	1.04
ρa_1^{3pr}	0.64
$\pi\pi$	0.38
πa_1^{3pr}	0.46
$a_1^{1pr} \rho$ and $a_1^{1pr} a_1^{1pr}$	0.30
πa_1^{1pr}	0.23
$a_1^{3pr} a_1^{3pr}$	0.13
$a_1^{3pr} a_1^{1pr}$	0.11
Combined	2.33

Expected sensitivities in standard deviations to distinguish between a CP-even and odd $H\tau\tau$ coupling

Results are displayed for the individual decay modes, the combined $\tau_\mu \tau_h$ and $\tau_h \tau_h$ channel, and the overall combination